Takeshi Kita,[1] Allen C. Clermont,[1] Nivetha Murugesan,[1] Qunfang Zhou,[1]
Kimihiko Fujisawa,[2] Tatsuro Ishibashi,[2] Lloyd Paul Aiello,[1,3] and Edward P. Feener[1,4]

Plasma Kallikrein-Kinin System as a VEGF-Independent Mediator of Diabetic Macular Edema

Diabetes 2015;64:3588–3599 | DOI: 10.2337/db15-0317

This study characterizes the kallikrein-kinin system in vitreous from individuals with diabetic macular edema (DME) and examines mechanisms contributing to retinal thickening and retinal vascular permeability (RVP). Plasma prekallikrein (PPK) and plasma kallikrein (PKal) were increased twofold and 11.0-fold (both $P < 0.0001$), respectively, in vitreous from subjects with DME compared with those with a macular hole (MH). While the vascular endothelial growth factor (VEGF) level was also increased in DME vitreous, PKal and VEGF concentrations do not correlate ($r = 0.266$, $P = 0.112$). Using mass spectrometry–based proteomics, we identified 167 vitreous proteins, including 30 that were increased in DME (fourfold or more, $P < 0.001$ vs. MH). The majority of proteins associated with DME displayed a higher correlation with PPK than with VEGF concentrations. DME vitreous containing relatively high levels of PKal and low VEGF induced RVP when injected into the vitreous of diabetic rats, a response blocked by bradykinin receptor antagonism but not by bevacizumab. Bradykinin-induced retinal thickening in mice was not affected by blockade of VEGF receptor 2. Diabetes-induced RVP was decreased by up to 78% ($P < 0.001$) in Klkb1 (PPK)-deficient mice compared with wild-type controls. B2- and B1 receptor–induced RVP in diabetic mice was blocked by endothelial nitric oxide synthase (NOS) and inducible NOS deficiency, respectively. These findings implicate the PKal pathway as a VEGF-independent mediator of DME.

Diabetic macular edema (DME) is a leading cause of vision loss among working-aged adults, with a global prevalence of ~16% for people with history of diabetes mellitus (DM) of ≥20 years (1). This sight-threatening disease is characterized by thickening of the macula due to the accumulation of intraretinal and/or subretinal fluid and exudates, with associated impairment of central visual acuity. The pathogenesis of DME has been primarily attributed to retinal vascular hyperpermeability, which results in extravasation of plasma proteins and lipids into the macula, and increased hydrostatic pressure across the blood-retinal barrier (2). Although DME can occur at any stage of diabetic retinopathy (DR), its incidence is higher in patients with more advanced stages of the disease, including severe nonproliferative DR (NPDR) and proliferative DR (PDR) (3). These observations suggest that underlying retinal pathologies associated with DR, in combination with systemic factors, including hyperglycemia, hypertension, and dyslipidemia, contribute to DME (4).

Vascular endothelial growth factor (VEGF) contributes to the macular thickening and visual impairment associated with DME (5). VEGF concentrations in vitreous and aqueous humor are increased in PDR and DME compared with controls without advanced DR (6–8). Intravitreal injection of therapies that block VEGF actions, including ranibizumab, bevacizumab, and aflibercept, have emerged as effective primary treatments for DME (9). However, most studies to date (10,11) have reported that a significant proportion of DME patients, up to ~50%, do not fully respond to anti-VEGF therapy.

DR exhibits aspects of inflammation, including vascular hyperpermeability, immune cell recruitment, and elevated expression of proinflammatory cytokines, which have been implicated in the development and progression of retinal

[1]Joslin Diabetes Center, Harvard Medical School, Boston, MA
[2]Department of Ophthalmology, Graduate School of Medical Sciences, Kyushu University, Higashi-ku, Fukuoka City, Japan
[3]Beetham Eye Institute, Department of Ophthalmology, Harvard Medical School, Boston, MA
[4]Department of Medicine, Harvard Medical School, Boston, MA
Corresponding author: Edward P. Feener, edward.feener@joslin.harvard.edu.

Received 6 March 2015 and accepted 3 May 2015.

This article contains Supplementary Data online at http://diabetes.diabetesjournals.org/lookup/suppl/doi:10.2337/db15-0317/-/DC1.

See accompanying article, p. 3350.

pathologies (4). The kallikrein-kinin system (KKS) contributes to the inflammatory response to vascular injury and is a clinically significant mediator of vasogenic edema associated with hereditary angioedema (12,13). Reports from our group and others (14–18) have demonstrated that the KKS mediates vascular hyperpermeability, leukostasis, cytokine production, and retinal thickening in rodent models of DR. The proinflammatory effects of the KKS are mediated by plasma kallikrein (PKal), a serine protease derived from the abundant circulating zymogen plasma prekallikrein (PPK). Zymogen activation by FXIIa cleaves PPK into disulfide-linked heavy and light chains of catalytically active PKal, which in turn cleaves FXII to FXIIa to provide positive feedback and amplification of the KKS. The physiological mechanisms that mediate FXII and PPK activation are not fully understood; however, hemorrhage, activated platelets, and unfolded proteins (19–21) have been shown to activate the KKS. PKal cleaves its substrate high–molecular-weight kininogen (HK) to release the nonapeptide hormone bradykinin (BK). BK activates the BK B2 receptor (B2R) and is also proteolytically processed by carboxypeptidase N into des-Arg^9-BK (DABK), which is a BK B1 receptor (B1R) agonist (22). Both B1R and B2R are G-protein–coupled receptors that are highly expressed in the retina (23), and retinal expression of B1R is increased in DM (15,16). While the plasma KKS has been implicated in DR (24,25), the levels of KKS components in DME vitreous and mechanisms that mediate the effects of the KKS on retinal vascular permeability (RVP) and retinal thickening are not yet available.

In this report, we quantified KKS components and VEGF and used mass spectrometry–based proteomics to characterize vitreous samples from patients with DME. The effects of the KKS on retinal vascular function and thickness in diabetic rodents were examined using Klkb1, inducible nitric oxide synthase (iNOS), and endothelial NOS (eNOS) knockout mice and measurements of retinal B1R and B2R responses. Our results suggest that upregulation of the intraocular KKS may contribute to a VEGF-independent mechanism of DME.

RESEARCH DESIGN AND METHODS

Analysis of KKS Components, VEGF, and Proteome in Human Vitreous

Human vitreous samples were obtained from patients undergoing pars plana vitrectomy during surgery for macular hole (MH) and various stages of DR, including DME without any PDR findings such as preretinal proliferative membrane or neovascularization, and PDR without vitreous hemorrhage. VEGF levels were measured by ELISA (R&D Systems, Minneapolis, MN). Undiluted vitreous samples were separated by SDS-PAGE (vitreous volumes used: 5, 1, and 1 μL for PPK/PK, FXII/FXIIa, and Kininogen Heavy Chain [HC], respectively) and immunoblotted using primary antibodies against Kallikrein 1B (catalog #NBP1–87711; Novus Biologicals), FXII (anti-FXII HC, catalog #ab1007; Abcam), HK (anti-Kininogen HC [2B5], catalog #sc-23914; Santa Cruz Biotechnology). Results were visualized by enhanced chemiluminescence (20× LumiGLO; Cell Signaling Technology) and quantified using ImageJ, version 1.48 (National Institutes of Health), image analysis software. Western blot analysis of purified standards for PPK, FXII, and HK (Enzyme Research Laboratories) were also performed along with vitreous samples for the quantification. Vitreous proteomics was performed by tandem mass spectrometry, as described previously (26,27). Protein abundance was calculated using total spectral counting for each protein from the X! Tandem search results. For statistical comparisons between groups, samples that did not have two unique peptides for an identified protein were assigned a value of 1, corresponding to half of the minimum detection threshold of two unique peptides. Protein identifications (IDs) were converted to gene symbols using DAVID (28). This study was carried out with approval from the institutional review board and was performed in accordance with the ethical standards of the 1989 Declaration of Helsinki.

Animal Models and DM Induction

DM was induced by intraperitoneal injection of streptozotocin (STZ; Sigma-Aldrich, Milwaukee, WI) in male Sprague-Dawley rats (8 weeks old, Taconic Farms, Hudson, NY). Blood glucose values >250 mg/dL were considered diabetic. Experiments were conducted after 4 weeks of DM and compared with age-matched nondiabetic (NDM) controls.

Klkb1 knockout mice were described previously (29) and backcrossed against C57BL/6 mice for nine generations. Mice deficient in eNOS (B6.129P2-*Nos3*^{tm1Unc}/J) and iNOS (B6;129P2-*Nos2*^{tm1Lau}/J) and age-matched wild-type (WT) mice were purchased from The Jackson Laboratory (Bar Harbor, ME). DM was induced by intraperitoneal injection of STZ (45 mg/kg) every 24 h for 5 days. Mice with blood glucose levels >250 mg/dL were considered diabetic, and retinal measurements were performed on eNOS$^{-/-}$ and iNOS$^{-/-}$ mice at 8 weeks and on Klkb1$^{-/-}$ mice at 12 weeks of DM duration. Approval for the animal protocols was obtained from the Joslin Diabetes Center Institutional Animal Care and Use Committee. The procedures adhered to the guidelines from The Association for Research in Vision and Ophthalmology for animal use in research.

Measurements of RVP

Intravitreal injections of BK, DABK, and VEGF in rats were performed, and RVP was measured by vitreous fluorophotometry, as described previously (14). Briefly, the eyes were dilated and received intravitreal injection of BK (2 μmol/L; Sigma-Aldrich), DABK (2 μmol/L; Sigma-Aldrich), VEGF (0.02 ng/mL in vitreous) (rhVEGF 165; R&D Systems), or PBS. Ten minutes after the injection, the rats were infused with 10% sodium fluorescein (300 μL/kg) through a jugular vein catheter. After an additional 30 min, vitreous fluorescein levels were measured by vitreous fluorophotometry, as previously described (19). L-N^G-nitro-L-arginine methyl

ester (L-NAME) (100 mg/L), a nitric oxide synthesis inhibitor, was administered for 3 days prior to intravitreal injection via the drinking water. B1R antagonist des-Arg^{10}-Hoe140 and B2R antagonist Hoe140 (AnaSpec, Fremont, CA) were systemically administered via micro-osmotic pump (subcutaneously implanted in the dorsal flank; model 1003D; ALZET) at 1 μg/μL/h, initiated 24 h prior to intravitreal injection. Bevacizumab (12.5 μg/eye) was administered to rats by intravitreal injection in the absence or presence of VEGF or human vitreous. RVP in mice was measured using Evans Blue permeation (30). Mice were anesthetized, received intravitreal injections with 1 μL of 20 μmol/L BK or DABK or PBS, and infused with Evans Blue dye (45 mg/kg) through a catheter in the jugular vein. The dye was allowed to circulate for 1 h prior to sacrifice. After tissue fixation by 10% formalin, the eyes were enucleated and the retinas were extracted. Retinas were incubated with dimethyl formamide overnight at 72°C after drying, and the resultant supernatant was used to determine Evans Blue dye content (14). Results were normalized by retinal tissue weight and levels of the dye in plasma.

Measurement of Retinal Thickness by Spectral Domain-Optical Coherence Tomography

Retinal thickness was analyzed using a commercial spectral domain-optical coherence tomography (SD-OCT) system (840SDOCT System; Bioptigen, Durham, NC), as previously described (14). Animals received intravitreal injections, as described above. In addition, a subset of mice received intravitreal injections with VEGF and DC101 (GeneTex). In brief, rectangular volumes of each retina were obtained consisting of 1,000 A-scans by 100 B-scans over a 1.5 × 1.5 mm area centered upon the optic nerve head. Thickness was measured at 500 μm relative to the optic nerve head. A total of four caliper measurements were taken from each site, corresponding to the temporal, nasal, superior, and inferior quadrants of the retina. The measurements from the retinal pigmented epithelium to the nerve fiber layer were averaged to produce a single thickness value for each retina.

Cell Culture and Western Blot Analysis

Bovine eyes were obtained from a local abattoir, and neonate rats were purchased from Taconic (Germantown, NY). Bovine retinal capillary endothelial cells (BRECs) and astrocytes were isolated as previously reported (31,32). Astrocytes were confirmed by immunocytochemical staining for glial fibrillary acidic protein. Cultured BRECs and ASCs were used between passages 4 to 7 and 3 to 5, respectively. Subconfluent cells were starved with endothelial basal medium (Lonza, Walkersville, MD) for BRECs or DMEM/F-12 for ASCs, containing 1% calf serum and subsequently treated with DMEM containing 25 mmol/L glucose, which were refed with fresh media every 24 h for up to 5 days. Total cell lysates were extracted, and Western blot analysis was performed to detect B1R (Enzo Life Sciences, Farmingdale, NY), B2R (BD Biosciences, San Jose, CA), iNOS (Ab3523; Abcam), eNOS (antiphospho-eNOS [Ser1177], catalog #9571, and anti-eNOS, catalog #9572; Cell Signaling Technology), and GAPDH (Santa Cruz Biotechnology). Band intensities were quantified and expressed as the percentage ratio to GAPDH.

Statistics

All results were expressed as the mean ± SEM. The statistical significance of differences between groups was analyzed by two-tailed Student *t* test or Mann-Whitney *U* test. For in vivo experiments, group conditions were compared by one-way ANOVA using the Fisher least significant differences method for pairwise multiple comparisons. Differences were considered significant at $P < 0.05$.

RESULTS

Intravitreal KKS and VEGF in DME

Concentrations of KKS components and VEGF were measured in vitreous samples obtained by pars plana vitrectomy from patients with NPDR and DME (NPDR/DME), PDR, and MH (Supplementary Table 1). Within the PDR group, patients with combined PDR and DME versus those with PDR alone were not examined separately. Levels of PPK, FXII, and HK in undiluted vitreous samples were quantified by Western blotting and comparison of band intensities for corresponding purified protein standards (Fig. 1*A*–*E* and Supplementary Fig. 1*A* and *B*). Western blots of PPK and FXII revealed bands at ~75 and 50 kDa, which are consistent with the zymogens and HCs of the activated enzymes, respectively (Supplementary Fig. 1*A* and *B*). PPK levels were significantly elevated in the vitreous from eyes with DME and PDR by approximately twofold compared with MH ($P < 0.001$) (Fig. 1*B*). Activated PKal, measured by HC levels, was increased by 11.0- and 10.4-fold, respectively, in the DME and PDR samples, relative to the average MH level (Fig. 1*C*). Comparable increases in FXII and HK HC were observed in NPDR/DME and PDR compared with MH vitreous (Fig. 1*D* and *E* and Supplementary Fig. 1*B*). In addition, increased levels of carboxypeptidase N were detected in vitreous from patients with NPDR/DME and PDR compared with MH, and hemoglobin was increased in PDR vitreous (Supplementary Fig. 1*C*). Concentrations of VEGF in vitreous with NPDR/DME (1,063.1 ± 285.3 pg/mL, $P < 0.0001$, $n = 20$) and PDR (1,107.8 ± 260.7 pg/mL, $P < 0.0001$, $n = 24$) were elevated compared with VEGF in vitreous from MH, which was below the detection limit for the assay (Fig. 1*F*).

The correlations among levels of KKS components and VEGF in the vitreous from NPDR/DME and MH subjects were examined. PPK levels correlated with its substrate HK (PPK vs. HK: $r = 0.656$, $P < 0.001$; Supplementary Fig. 2*A*) but not with VEGF (VEGF vs. PPK: $r = 0.168$, $P = 0.499$; Fig. 1*G*). DME vitreous samples were ranked in order of their VEGF concentrations, and the levels of PKal in these samples are shown in Fig. 1*H*. PKal and VEGF levels in DME vitreous do not correlate ($r = 0.266$,

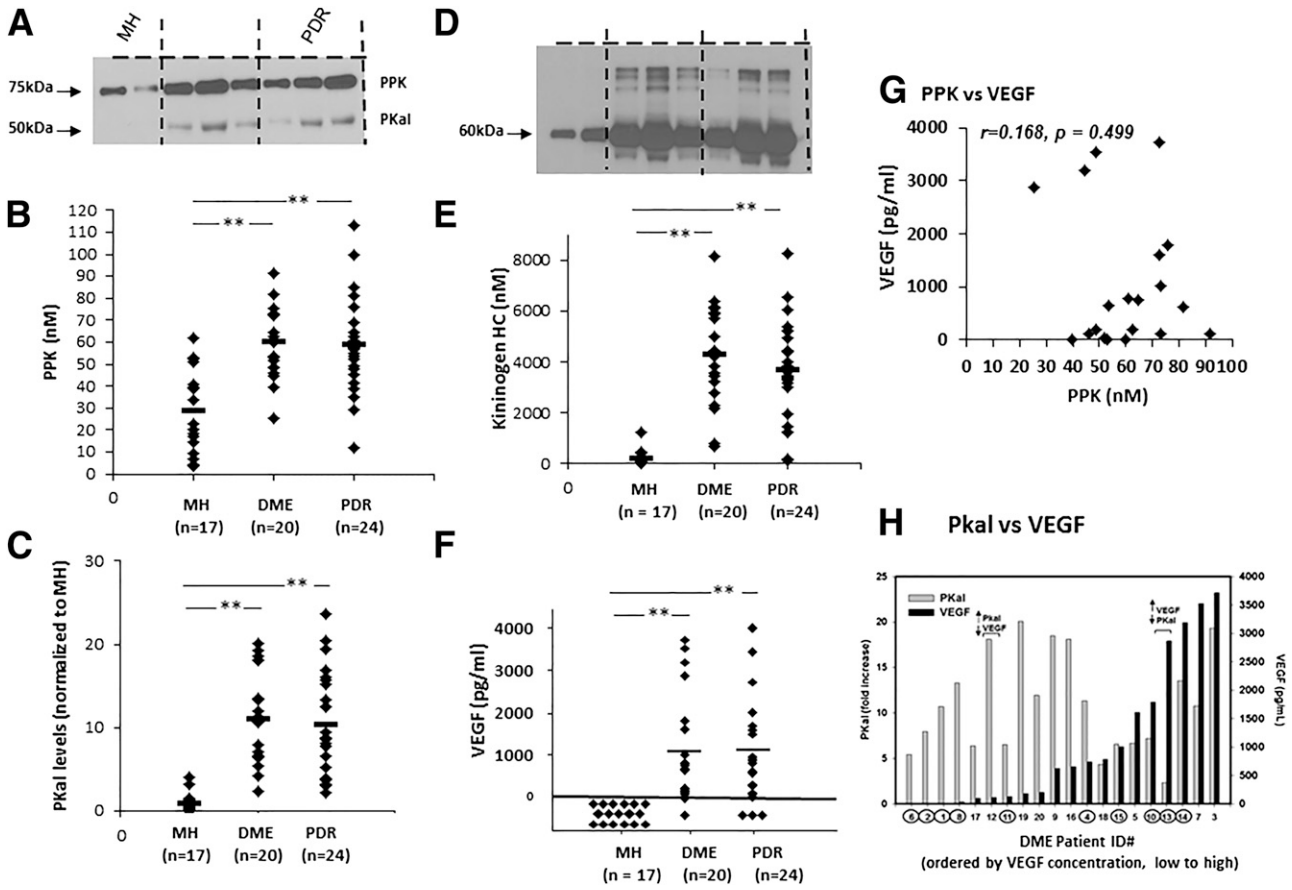

Figure 1—Concentrations of KKS components and VEGF in human vitreous. *A* and *D*: Western blot analyses of PPK, PKal, and HK in vitreous samples from subjects with MH, DME, and PDR. Concentrations of PPK (*B*), PKal (*C*), HK (*E*), and VEGF (*F*) in undiluted vitreous samples. *G*: Correlations of PPK and VEGF are $r = 0.168$, $P = 0.499$ in DME vitreous samples. Levels of PKal in DME vitreous samples are ranked in ascending order of VEGF concentration. *H*: Samples used for proteomics are circled. $^{**}P < 0.0001$ vs. MH (Mann-Whitney *U* test).

$P = 0.112$). Moreover, these results revealed three groups of samples, including samples (ID #6–20) with high PKal and low VEGF, samples (ID #9–10 and 14–3) with elevated levels of both VEGF and PKal, and sample ID #13 with high VEGF and low PKal (Fig. 1*H*). Similarly, the correlations among the other KKS were higher than their correlations with VEGF (PPK vs. FXII: $r = 0.329$, $P = 0.157$; FXII vs. HK: $r = 0.592$, $P = 0.006$; VEGF vs. FXII: $r = 0.130$, $P = 0.585$; and VEGF vs. HK: $r = 0.020$, $P = 0.934$) (Supplementary Fig. 2*B–E*).

Vitreous Proteome in DME

Vitreous proteomic abnormalities have been implicated in DME (19,26). We used proteomics to further characterize the DME vitreous proteome and correlations with PPK and VEGF concentrations. Mass spectrometry–based proteomics was performed on 10 vitreous samples from DME patients and on 5 vitreous samples from MH patients. DME samples used for proteomics are indicated in Fig. 1*H*. The list of proteins and corresponding numbers of spectral/peptide counts for each sample are shown in Supplementary Table 2. We identified a total of 167 proteins, including 39 proteins detected only in DME vitreous and 10 proteins detected only in MH vitreous (Fig. 2*A*). This proteome contained 138 proteins that were identified in three or more independent vitreous samples. The numbers of total spectral-peptide matches were used to compare the abundance of these proteins between DME and MH samples. Thirty proteins were increased in DME (fourfold or more, $P < 0.001$, vs. MH) in vitreous from DME compared with MH samples (Table 1). The concentrations of PKal and VEGF in the 10 DME vitreous samples used for proteomics are indicated in Fig. 1*H*. Correlation analyses for spectral-peptide counts for these proteins and PPK and VEGF concentrations were performed. This analysis shows that most of the proteins in Table 1 displayed higher correlative *R* values for comparison with PPK concentrations than with VEGF concentrations (Fig. 2*B*). In addition, we show that the concentrations of PPK and total protein correlate in DME vitreous ($r = 0.618$, $P = 0.001$), whereas VEGF concentration do not correlate with total vitreous protein concentration ($r = 0.115$, $P = 0.499$) (Fig. 2*C* and *D*). These data reveal marked heterogeneity in the concentrations of KKS components, VEGF, and total protein in vitreous samples from patients with NPDR and DME.

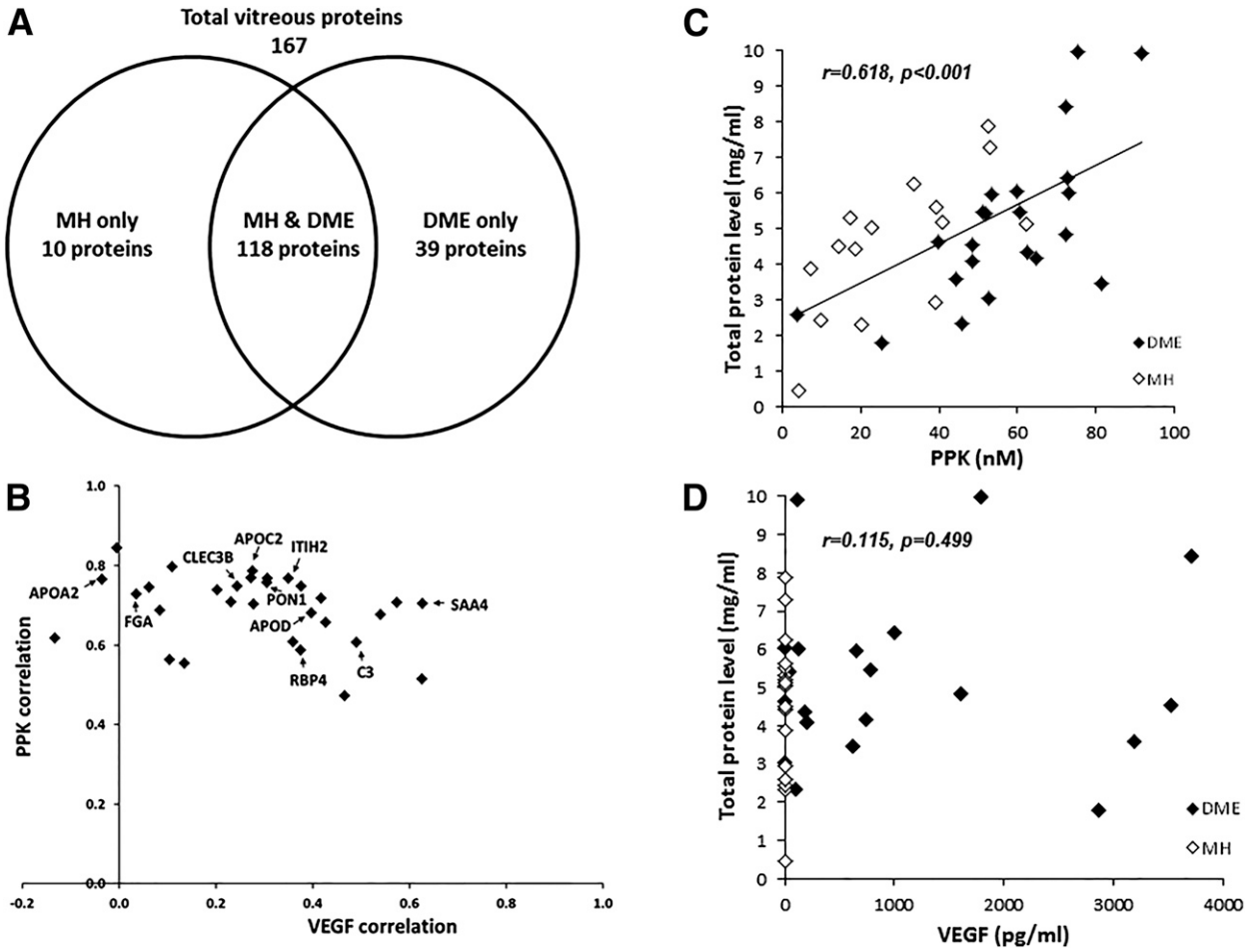

Figure 2—Proteomics of DME vitreous and correlations with PKal and VEGF. *A*: Venn diagram summary of total proteins identified in DME and MH vitreous by mass spectroscopy–based proteomics. Correlations of proteins that are increased (more than threefold, $P < 0.001$) in DME vitreous with respective intravitreal PPK and VEGF concentrations. *B*: The 10 proteins that displayed the largest fold increase in DME compared with MH vitreous are labeled with gene symbols. Correlations of total vitreous protein concentration with PPK (*C*) and VEGF (*D*) concentrations.

Retinal B1R and B2R Expression in DM

To further characterize the effects of DM on the intraocular KKS, we examined retinal B1R and B2R expression in rats with 4 weeks of STZ-induced DM and age-matched NDM controls. B1R levels were increased by 2.2-fold in DM rats compared with NDM controls ($P = 0.001$), whereas B2R was similarly expressed in DM and NDM rat retinas (Supplementary Fig. 3*A*). Next, we examined the effects of extracellular glucose concentration on B1R and B2R levels in cultured BRECs and rat brain astrocytes. B1R expression was increased by twofold to threefold in BRECs and astrocytes cultured in media containing 25 mmol/L glucose compared with cells maintained in media containing 5 mmol/L glucose ($P < 0.01$, $n = 3$) (Supplementary Fig. 3*B* and *C*). In contrast, incubation of BRECs and astrocytes in the presence of 25 mmol/L glucose did not alter B2R levels.

Effects of BK and DABK on RVP and Thickness

Since the effects of the KKS on vascular permeability are primarily mediated by the BK system (22), we examined the effects of BK and DABK on RVP and retinal thickness in rats with 4 weeks of DM along with age-matched NDM controls. The effects of intravitreal injection of BK and DABK in DM rats were examined over a time course of 40 min to 48 h (data not shown). BK rapidly increased RVP (at 40 min), and this response gradually decreased at later time points. In contrast, the effect of DABK on RVP was delayed and was highest at 48 h after intravitreal injection. The effects of BK and DABK on RVP were further characterized at 40 min and 48 h, respectively. We observed a small increase in RVP in DM rats compared with NDM rats at 40 min ($P < 0.0001$) and 48 h ($P < 0.0001$) after intravitreal injections with PBS vehicle. Intravitreal injection of BK increased RVP after 40 min in both NDM rats (3.6-fold, $P = 0.001$) and DM rats (2.1-fold, $P < 0.0001$) compared with PBS-injected controls, and levels returned to baseline levels at 48 h postinjection (Fig. 3*A*). In contrast, intravitreal injection of DABK did not affect RVP in the short term at 40 min but increased RVP at 48 h postinjection in DM rats (twofold, $P < 0.0001$), an effect

Table 1—Correlations of proteins increased in DME vitreous with concentrations of PPK and VEGF

Gene symbol	Description	Average DME/MH	PPK correlation	VEGF correlation	Estimated plasma protein concentration*
FGA	Fibrinogen alpha chain	38.6	0.728	0.036	130 pg/mL
SAA4	Serum amyloid A4, constitutive	18.7	0.705	0.628	30 μg/mL
RBP4	Retinol binding protein 4, plasma	14.5	0.587	0.375	580 μg/mL
APOD	Apolipoprotein D	10.1	0.681	0.398	82 μg/mL
PON1	Paraoxonase 1	10.1	0.758	0.305	7.7 μg/mL
CLEC3B	C-type lectin domain family 3, member B	9.2	0.748	0.245	58 μg/mL
APOA2	Apolipoprotein A-II	9.2	0.766	−0.035	750 μg/mL
APOC2	Apolipoprotein C-II	8.0	0.769	0.272	240 μg/mL
ITIH2	Inter-alpha-trypsin inhibitor heavy chain 2	7.6	0.767	0.350	21 μg/mL
C6	Complement component 6	7.4	0.606	0.490	3,700 ng/mL
AFM	Afamin	7.1	0.747	0.376	320 μg/mL
KNG1	Kininogen 1	7.0	0.709	0.232	28 μg/mL
F2	Coagulation factor II (thrombin)	6.8	0.718	0.418	27 μg/mL
C8G	Complement component 8, gamma polypeptide	6.8	0.845	−0.004	1.1 μg/mL
CFH	Complement factor H	6.8	0.738	0.203	57 μg/mL
C7	Complement component 7	6.6	0.745	0.062	2.6 μg/mL
ITIH4	Inter-alpha-trypsin inhibitor heavy chain family, member 4	6.5	0.677	0.541	42 μg/mL
VTN	Vitronectin	6.1	0.656	0.427	35 μg/mL
HP	Haptoglobin	6.0	0.767	0.306	210 μg/mL
APOA1	Apolipoprotein A-I	5.7	0.796	0.110	310 μg/mL
LRG1	Leucine-rich alpha-2-glycoprotein 1	5.3	0.514	0.626	2.7 μg/mL
RARRES2	Retinoic acid receptor responder (tazarotene induced) 2	4.8	0.563	0.105	570 ng/mL
C3	Complement component 3	4.7	0.786	0.276	260 μg/mL
PLG	Plasminogen	4.6	0.707	0.575	25 μg/mL
ITIH1	Inter-alpha-trypsin inhibitor heavy chain 1	4.5	0.608	0.359	24 μg/mL
SERPINF2	Serpin peptidase inhibitor, clade F (alpha-2 antiplasmin, pigment epithelium derived factor), member 2	4.3	0.472	0.466	12 μg/mL
APOH	Apolipoprotein H (beta-2-glycoprotein 1)	4.3	0.617	−0.133	78 μg/mL
AHSG	Alpha-2-HS-glycoprotein	4.2	0.687	0.085	82 μg/mL
ITIH3	Inter-alpha-trypsin inhibitor heavy chain 3	4.1	0.553	0.135	2 μg/mL
A1BG	Alpha-1-B glycoprotein	4.0	0.703	0.278	50 μg/mL

*Estimated protein concentrations in human plasma are from Farrah et al. (37).

not observed at 48 h in NDM controls. The effects of BK and DABK on RVP in DM rats were blocked by Hoe140 (B2R antagonist) and des-Arg^{10}-Hoe140 (B1R antagonist) administered by subcutaneously implanted mini-osmotic pumps (Fig. 3*B*). The effects of intravitreal injection of VEGF on RVP were also investigated. VEGF increased RVP by 2.6-fold compared with vehicle-injected eyes at 40 min (P = 0.004), and this response returned to baseline at 48 h postinjection (Fig. 3*C*). The effect of VEGF on RVP measured at 40 min postinjection was blocked by coadministration with bevacizumab, but not by combined B1R/B2R antagonism.

The effects of intravitreal injection of BK and DABK on retinal thickness and retinal vessels in DM rats were examined by SD-OCT imaging at 6, 24, and 48 h postinjection compared with baseline. Representative B-scans show retinal structure at 24 and 48 h after BK and DABK injections, respectively, compared with vehicle-injected eyes (Fig. 3*D*).

Intravitreal injection of saline vehicle produced a small increase in retinal thickness at 24 and 48 h postinjection (5.46% and 5.81% increase, respectively; $P < 0.05$, n = 5). Intravitreal injection of BK rapidly increased the retinal thickness at 6 and 24 h postinjection (20.1% increase,

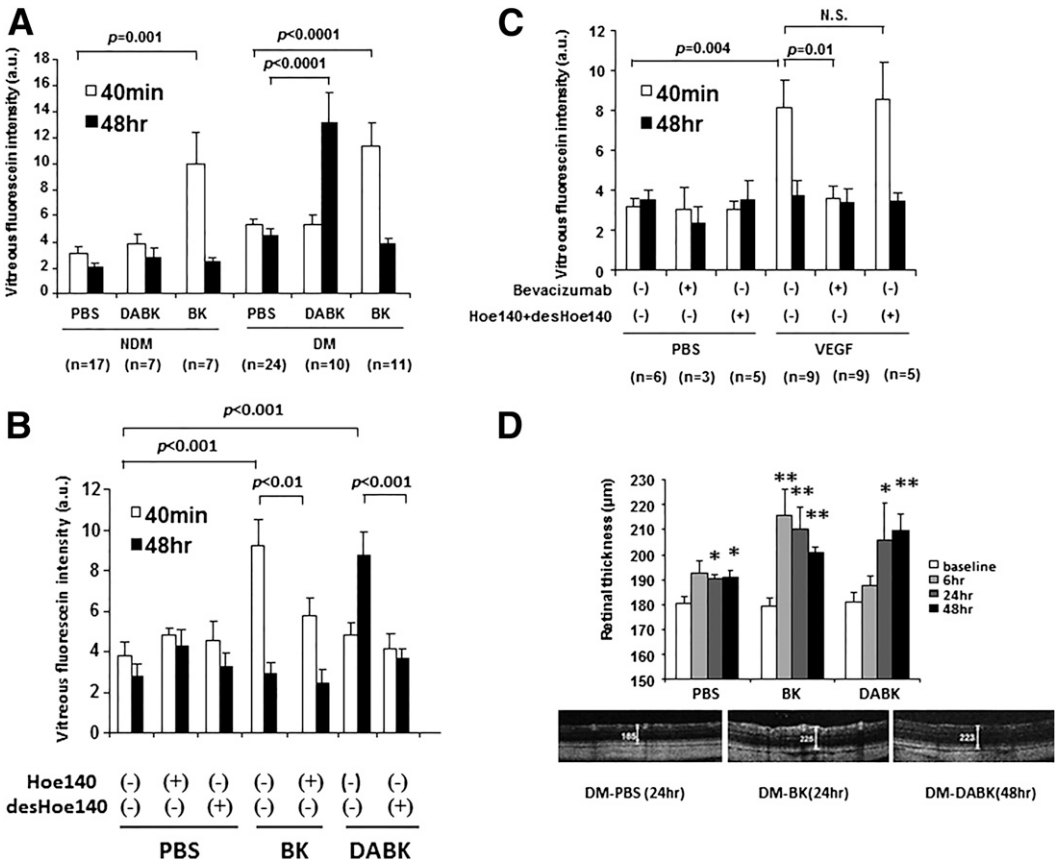

Figure 3—Effects of intravitreal injection of BK and DABK on RVP and retinal thickness in diabetic rats. Rat with 4 weeks of STZ-induced DM and age-matched NDM controls received intravitreal injections with BK (final concentration 2 μmol/L), DABK (final concentration 2 μmol/L), and saline vehicle (PBS), as indicated. *A–C*: RVP was measured at 40 min and 48 h after intravitreal injection by vitreous fluorophotometry. Rats were pretreated with Hoe140 or des-Arg^{10}-Hoe140 (desHoe140) (1 μg/kg/day) prior to intravitreal injections, as shown in panels *B* and *C*. Cointravitreal injections with bevacizumab were performed in panel *C*. *D*: Representative SD-OCT B-scan images of rat retinas following intravitreal injections with PBS, BK, and DABK. Retinal thickness was quantified by SD-OCT. **P* < 0.05, ***P* < 0.01 vs. baseline. a.u., arbitrary units.

$P < 0.01$), and thickness tended to decrease at 48 h but was still thicker than baseline (11.9% increase, $P < 0.01$). DABK increased retinal thickness at 24 h (13.7%) and 48 h (15.8%) postinjection (Fig. 3*D*).

Effects of Human Vitreous on RVP in Rats

The potential effects of VEGF and BK peptides in human vitreous on the RVP were examined in the rat model of RVP described above. We selected two human vitreous DME samples, as indicated in Fig. 1*H*, patient ID #12, with relatively high PKal and low VEGF (PK↑ vit; PPK 91.6 nmol/L [18.1-fold increase in PKal], VEGF 114 pg/mL) and patient ID #13, with low PKal and high VEGF (VEGF↑ vit; PPK 25.2 nmol/L [2.3-fold increase in PKal], VEGF 2,864 pg/mL), and a control MH vitreous with low levels of both PKal and VEGF. Ten microliters of human vitreous fluid was injected into the vitreous of DM rats in the presence or absence of coinjections with bevacizumab or the combination of Hoe140 and des-Arg^{10}-Hoe140. At 40 min postinjection, PK↑ vit did not increase RVP, whereas VEGF↑ vit significantly enhanced RVP (1.41-fold, $P < 0.05$) compared with vitreous from the MH patient. The VEGF↑ vit–induced response was blocked by bevacizumab ($P < 0.01$) but not affected by Hoe140/des-Arg^{10}-Hoe140 (Fig. 4*A*). In contrast, at 48 h, RVP was increased by intravitreal injection of PKal↑ vit (1.6-fold, $P < 0.01$), which was suppressed by Hoe140/des-Arg^{10}-Hoe140 ($P < 0.01$), but not by bevacizumab (P = not significant [NS]). RVP that was increased at 40 min by intravitreal injection of VEGF↑ vit returned to baseline at 48 h postinjection (P = NS vs. MH) (Fig. 4*B*).

Effects of VEGF Receptor 2 Blockade on VEGF- and BK-Induced Retinal Thickening

Next, we tested the effects of VEGF receptor 2 (VEGFR2) blockade using DC101, an anti-VEGFR2 neutralizing antibody, on both VEGF- and BK-induced retinal thickening in WT C57BL/6 mice. Retinal thickness was measured by SD-OCT at baseline, and then mice received 1-μL intravitreal injections of VEGF (10 ng) and BK (20 μmol/L), in the absence or presence of DC101. At 24 h postinjection,

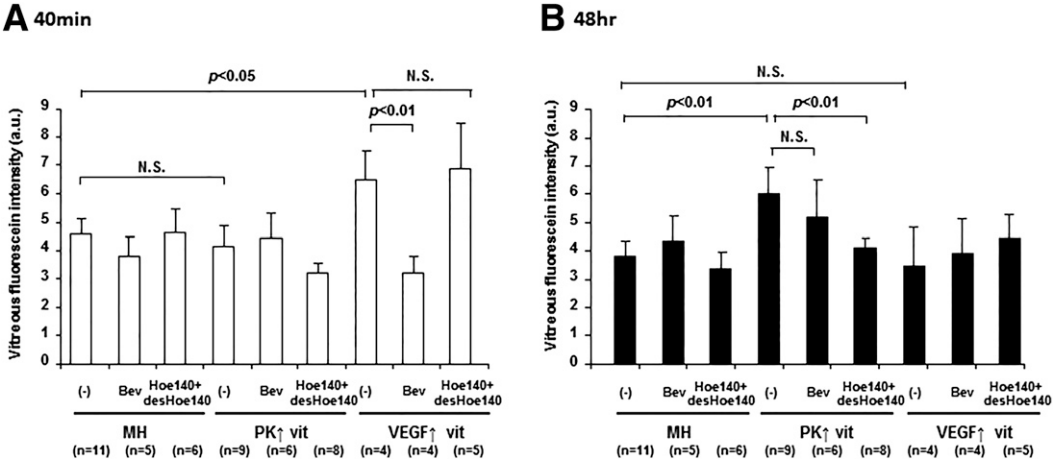

Figure 4—Effects of intravitreal injection of human DME vitreous on RVP in diabetic rats. Human vitreous samples, including DME patient ID #12 with relatively PK↑ vit (PPK 91.6 nmol/L [18.1-fold increase in PKal], VEGF 114 pg/mL), DME patient ID #13 with VEGF↑ vit (PPK 25.2 nmol/L [2.3-fold increase in PKal], VEGF 2,864 pg/mL), and control MH vitreous with low levels of both PKal and VEGF, were injected into rat vitreous. Coinjections were performed with Hoe140/desArg^{10}-Hoe140 (desHoe140) and bevacizumab (Bev), as indicated, and RVP was measured by vitreous fluorophotometry at 40 min (*A*) and 48 h (*B*) postinjection. a.u., arbitrary units.

retinal OCT measurements were repeated and the changes in thickness were determined. VEGF and BK similarly increased retinal thickness at 24 h by 15.2% and 13.6%, respectively ($P < 0.001$), compared with baseline (Fig. 5). Coinjection of DC101 at doses of 0.36 and 0.73 μg reduced VEGF-induced retinal thickness in a dose-responsive manner to 12.3% ($P < 0.001$) and 2.3% (P = NS) compared with baseline, respectively. Coinjection of 0.73 μg DC101 did not alter the effects of BK on retinal thickness (12.3%, $P < 0.001$) compared with baseline. Coinjection of DC101 did not alter retinal thickness in control eyes receiving PBS vehicle.

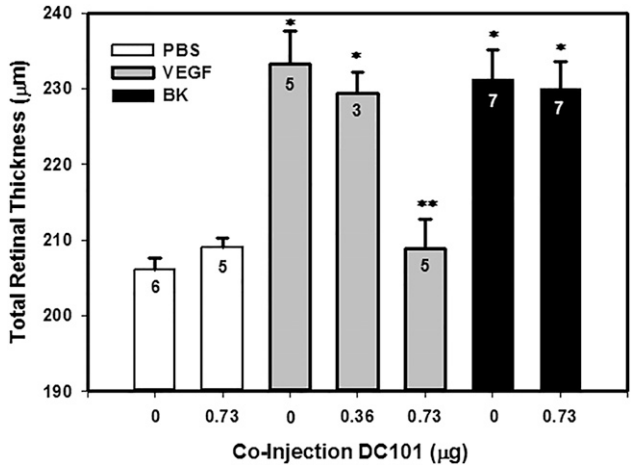

Figure 5—Effect of VEGFR2 blockade by DC101 on VEGF- and BK-induced retinal thickening. Retinal thickness was quantified by SD-OCT in WT mice at baseline and at 24 h after injection of PBS, VEGF, and BK with or without DC101 coinjections. VEGF and BK increased retinal thickness by 15.2% and 13.6% compared with baseline, respectively (*$P < 0.001$). Coinjection of VEGF with DC101 at 0.36 and 0.73 μg reduced VEGF-induced thickness by 14.7 (P = NS) and 90% (**$P < 0.001$) compared with VEGF alone, respectively. Coinjection of DC101 with BK had no effect on BK-induced thickness.

Effects of Klkb1 Deficiency on RVP and Retinal Thickness in Diabetic Mice

PPK, encoded by the Klkb1 gene, is the major source of proinflammatory levels of BK (22). Previous studies (14) have shown that PKal inhibition reduces RVP in diabetic rats. To further evaluate the role of PPK in DR, we examined the effects of Klkb1 deficiency on RVP and retinal thickness in WT and Klkb1$^{-/-}$ mice with 3 months of DM compared with NDM controls. Klkb1 deficiency did not alter body weight or blood glucose levels for DM or NDM groups, compared with age-matched WT littermate controls (Supplementary Fig. 4*A* and *B*). RVP, quantified using Evans Blue dye permeation, was increased in DM female (400 ± 63%, $P < 0.001$) and male (138 ± 31%, $P < 0.001$) WT mice compared with NDM WT controls (Fig. 6A and *B*). NDM WT and NDM Klkb1$^{-/-}$ mice of the same sex displayed similar RVP; however, we observed increased basal RVP in NDM male mice compared with NDM female mice. RVP in female DM Klkb1$^{-/-}$ mice was 78 ± 6% ($P < 0.001$) less than that in female DM WT mice (Fig. 6*A*). Similarly, the DM-induced increase in RVP in male Klkb1$^{-/-}$ mice was 58 ± 11% (P = 0.033) less than that in male DM WT mice (Fig. 6*B*).

Previous studies have reported that DM causes retinal neurodegeneration in mice (33). Using SD-OCT, we observed 3.4 ± 0.6% and 5.8 ± 0.8% decreases ($P < 0.01$) in retinal thickness in DM WT mice compared with NDM WT mice for female and male mice, respectively (Fig. 6*C* and *D*). The DM-associated decrease in retinal thickness in female Klkb1$^{-/-}$ mice was 1.6 ± 0.6%, which was thicker than that observed in female WT mice (204.9 ± 1.3 vs. 198.9 ± 1.2 μm, P = 0.002). In contrast, retinal thicknesses in male DM Klkb1$^{-/-}$ and DM WT mice were similar.

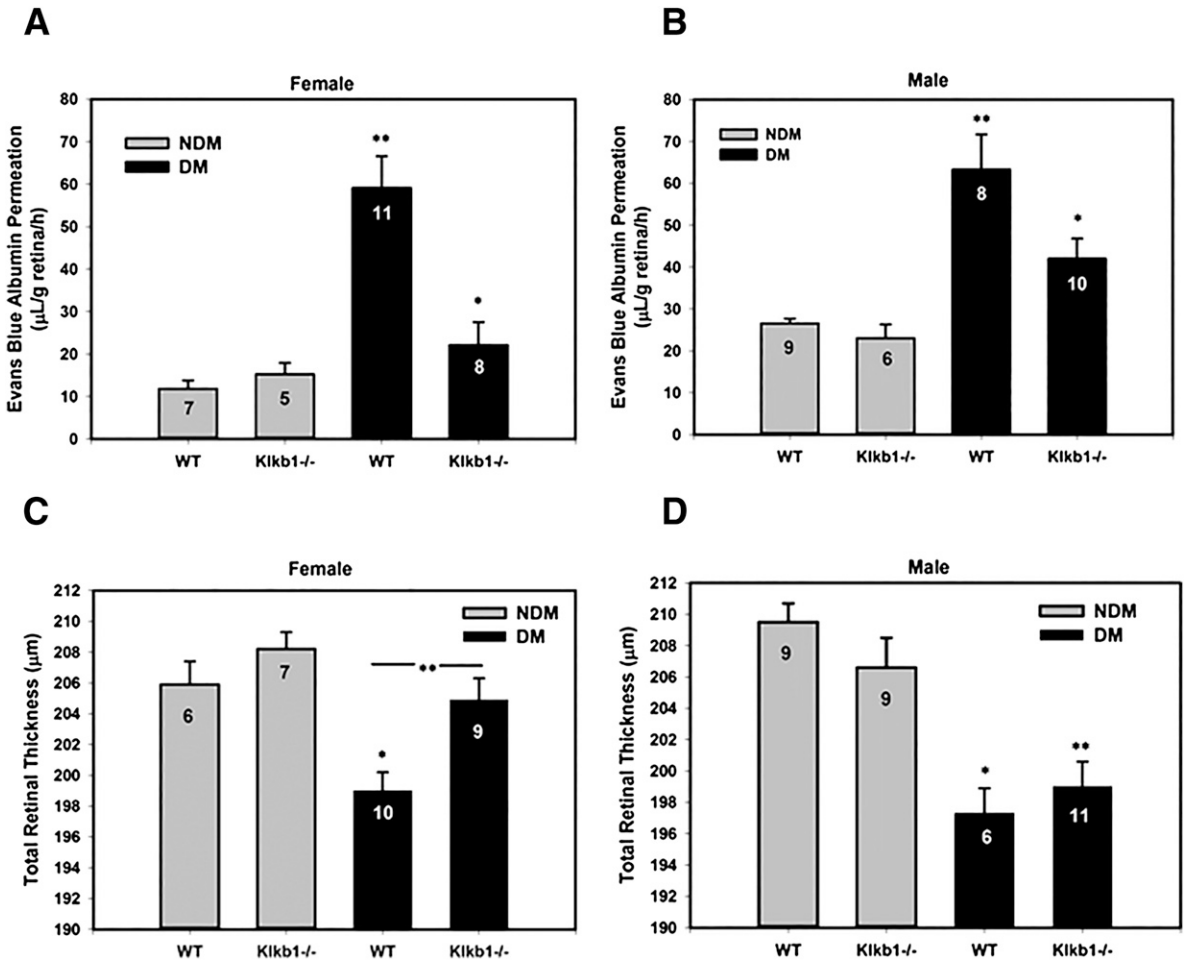

Figure 6—Effects of PPK deficiency (Klkb1$^{-/-}$) on RVP and retinal thickness in diabetic mice. DM increased RVP in female (*A*) and male (*B*) WT mice by 138 ± 31% and 400 ± 63%, respectively, compared with NDM controls (**P < 0.001). DM-induced RVP was decreased in Klkb1$^{-/-}$ mice by 58 ± 11% (*P = 0.033) in male mice and 78 ± 6% (*P < 0.001) in female mice. *C*: DM decreased retinal thickness in female WT mice by 3.4 ± 0.6% (*P = 0.001) and in female Klkb1$^{-/-}$ mice by 1.6 ± 0.6% (P = NS). The DM-associated decrease in retinal thickness in female Klkb1$^{-/-}$ mice was less than that observed in female WT mice (**P = 0.002). *D*: DM decreased total retinal thickness in male WT mice by 5.8 ± 0.8% (*P < 0.001) and in male Klkb1$^{-/-}$ mice by 3.7 ± 0.8% (**P = 0.004).

Involvement of eNOS and iNOS in BK- and DABK-Induced Vascular Permeability

Increased nitric oxide level contributes to the action and vascular permeability of BK in DR (17,34,35); however, the role of eNOS and iNOS in the effects of the KKS on the retina are not yet available. We examined the role of nitric oxide in BK- and DABK-induced RVP using L-NAME, which is hydrolyzed to N^G-nitro-L-arginine, a competitive inhibitor of eNOS, iNOS, and neuronal nitric oxide synthase. Systemic administration of L-NAME in DM rats blocked both the short-term effect of BK and the delayed effect of DABK on RVP (Fig. 7*A*). The effects of BK and DABK on eNOS phosphorylation were examined using BRECs. The addition of BK to the culture media increased eNOS phosphorylation at Ser1177 within 5 min, and maximum phosphorylation was observed after 30 min. In contrast, the incubation of BRECs with DABK did not alter eNOS phosphorylation at this site (Fig. 7*B*). The potential role of eNOS on BK-induced RVP was examined in WT and eNOS knockout mice in the absence and presence of 8 weeks of DM. In WT mice, BK increased RVP by 2.1-fold and 1.7-fold at 40 min after intravitreal injection compared with vehicle-injected eyes ($P < 0.01$) in NDM and DM mice, respectively, whereas intravitreal injection of BK did not alter RVP in eNOS-deficient mice (with/without DM) (Fig. 7*C*).

Since DABK effects on RVP were blocked by L-NAME but did not alter eNOS phosphorylation (Fig. 7*A* and *B*), we examined the effects of DABK on iNOS. Intravitreal injection of DABK increased iNOS expression in DM rat retinas compared with vehicle-injected eyes. This effect of DABK on iNOS was not observed in NDM rats (Fig. 7*D*). Furthermore, we examined the effect of DABK on iNOS protein levels in astrocytes in vitro. DABK induced increased expression of iNOS in astrocytes after 36 and 48 h of stimulation ($P < 0.01$ vs. untreated controls) (Fig. 7*E*). To examine

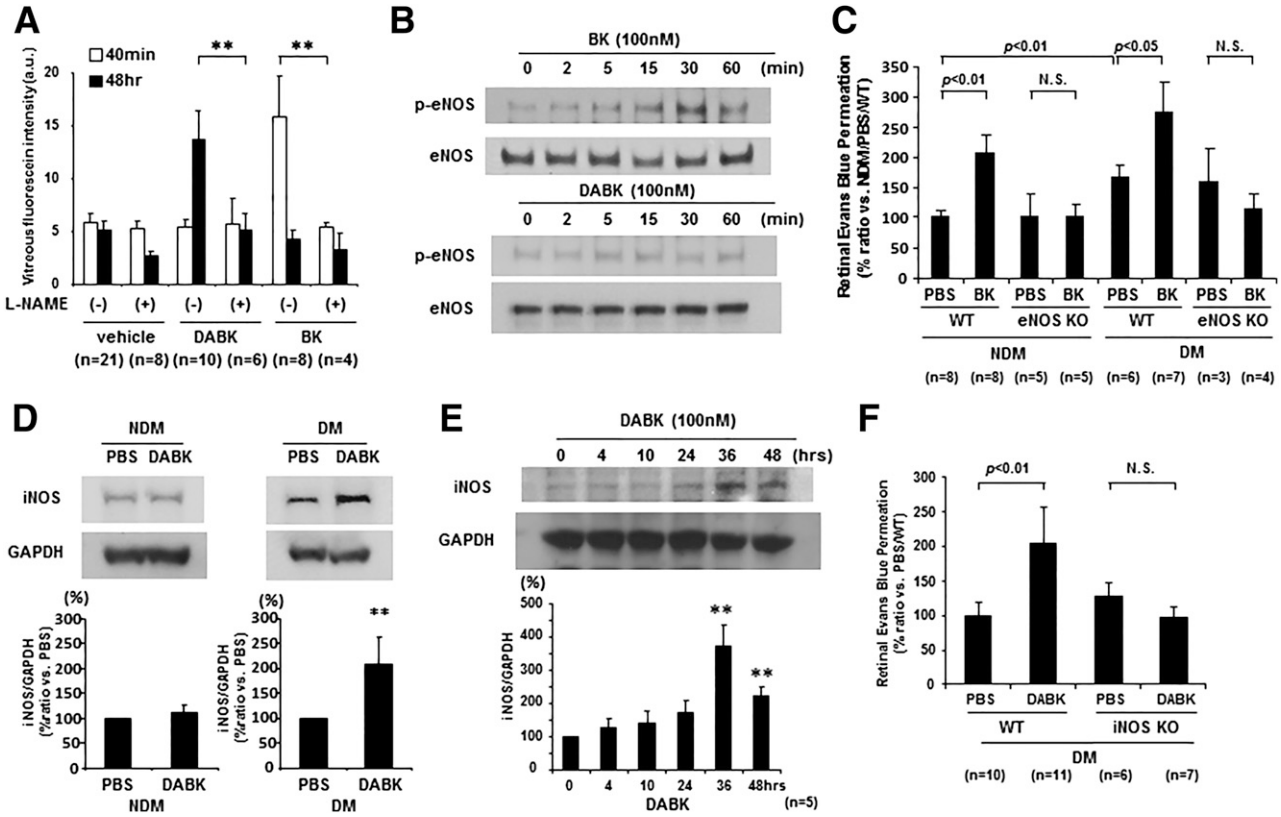

Figure 7—Role of NOS on RVP induced by BK peptides. *A*: Effect of L-NAME on DABK- and BK-induced RVP measured using vitreous fluorophotometry. *B*: Phosphorylation state of eNOS by BRECs in the presence of BK (100 nmol/L) or DABK (100 nmol/L). *C*: Effects of BK on RVP in WT and eNOS-deficient mice. *D*: Western blot analysis of iNOS normalized to GAPDH in diabetic and NDM mice injected with DABK. *E*: Effect DABK on iNOS levels in astrocytes. *F*: Effects of DABK on RVP in WT and iNOS-deficient mice. $^{**}P < 0.01$. a.u., arbitrary units; p, phosphorylated.

the potential role of iNOS on DABK-induced RVP, we examined the effects of intravitreal injection of DABK in DM iNOS knockout mice. Intravitreal injection of DABK increased RVP at 48 h postinjection in WT mice (2.0-fold vs. vehicle-treated WT mice, $P < 0.01$), whereas DABK did not alter RVP in iNOS-deficient mice (Fig. 7*F*).

DISCUSSION

In this report, we show that the KKS is activated in vitreous from DME patients. Vitreous from subjects with relatively high concentrations of PKal and low concentrations of VEGF induce RVP via the BK pathway, whereas VEGF mediates this response for vitreous with high VEGF concentrations and low PKal concentrations. These data demonstrate heterogeneity among a cohort of DME subjects in regard to vitreous protein composition and activity of vitreous fluid. Since KKS components are abundant plasma proteins, and PPK levels correlate with other abundant plasma proteins in the vitreous, it is likely that the increases in DME vitreous are due to plasma protein extravasation as a result of blood-retina barrier dysfunction. Indeed, the proteins that we identified to be increased in DME vitreous (Table 1) have been previously identified in human plasma (http://www.plasmaproteomedatabase.org) (36). The concentrations of these proteins in normal plasma have been estimated by Farrah et al. (37) using spectral counts and are listed in Table 1. We show that PPK, but not VEGF, concentrations correlate with most vitreous protein increases identified by proteomics and total vitreous protein concentration. Moreover, PKal concentrations are elevated in most DME vitreous samples, whereas VEGF displays a greater range of concentrations among these vitreous samples. Increased intraocular concentrations of VEGF have been attributed largely to retinal ischemia/hypoxia, and there is a known wide range of VEGF concentrations among DME vitreous samples (7,38). The wide variability among vitreous VEGF concentrations and the extent of retinal edema imply that additional factors may play important roles in mediating some cases of DME (9,19). Increased RVP and plasma protein extravasation in DR has been attributed to a variety of mechanisms, which are not limited to VEGF (2). Intravitreal injection of KKS components increases RVP and retinal thickening in diabetic animals (14,16,19). While BK generated from HK is a primary effector pathway of the KKS, the DME vitreous also contains components of the complement and coagulations systems, such as complement C3, thrombin, and plasminogen, which may contribute to proinflammatory

effects downstream of PKal and FXIIa (39). The temporal events and relative contributions of the VEGF and PKal pathways in DME may depend on the underlying retinal pathologies, such as levels of retinal ischemic, and the extent of vascular injury and inflammation. We propose that KKS extravasation in DR is mediated by multiple factors and that high levels of intraocular KKS activity exacerbates RVP, which overwhelms fluid resorptive mechanisms, resulting in retinal thickening. Moreover, our findings suggest that increased intraocular PKal may contribute to an incomplete or delayed response to anti-VEGF therapies for patients in whom intravitreal KKS activity is high. Additional VEGF-independent pathways and retinal structural changes such as disorganization of the retinal inner layers are also likely to contribute to the range of clinical responses observed after anti-VEGF treatment of DME (40–42).

Elevated nitric oxide production has been implicated in the pathogenesis of DR via multiple mechanisms (43). Mice deficient in eNOS display increased iNOS expression, nitric oxide levels, and DR compared with diabetic WT controls (35). Mice with iNOS deficiency are protected from DM-induced RVP and retinal capillary degeneration (44,45). B1R and B2R are expressed in vascular, glial, and neuronal cells, and the mechanisms that couple the KKS to nitric oxide production differ at the cellular level. BK stimulates eNOS phosphorylation in BRECs, whereas the B1R agonist DABK induces iNOS expression in astrocytes. Astrocytes are distributed on the surface of the inner retina, and retinal capillaries are surrounded by the astrocyte foot process, which can swell and release inflammatory cytokines that increase blood-retina barrier permeability (46). These findings suggest that the KKS may exert its effects on RVP by inducing nitric oxide production in both glial and vascular cells. We show that BK similarly induces RVP in DM and NDM rats, suggesting that B2R may contribute to RVP in the presence of KKS activation in the vitreous. In addition, we show that B1R levels and DABK responses in the retina are increased in diabetic rats compared with NDM controls. These findings are consistent with those of previous reports (15,16,47) showing that B1R mRNA expression and responses are increased in DM and inflammation. In DM, proinflammatory cytokines may contribute to increased DABK action via upregulation of B1R and iNOS expression, which could provide additive effects to the B2R/eNOS pathway on RVP (34). Although selective inhibition of B1R could potentially provide some protective effect for retinal dysfunction in DR, this approach would not address the potential contributions of B2R or effects mediated by PKal substrates other than HK (18,29). However, the blockade of PKal could reduce the proinflammatory effects of the intravitreal KKS while preserving the potential beneficial ocular effects of BK generated by tissue kallikrein (Klk1) (48).

Taken together, our results suggest that the PKal-mediated KKS exerts effects on DR at two levels. In the early stages of DR, a low level of KKS activation increases RVP via both retinal B1R and B2R. This DM-induced vascular hyperpermeability is blocked by Klkb1 deficiency and the administration of either a PKal inhibitor (14) or B1R antagonists (15,17). Although this early increase in RVP may contribute to the pathogenesis of DR, it is not sufficient to cause retinal thickening. The transition to retinal edema, including DME, appears to require further upregulation of vascular permeability factors, such VEGF and PKal, which are markedly increased in the vitreous during advanced stages of DR compared with DM alone (6). Since many individuals are not fully responsive to anti-VEGF DME therapy (10), PKal inhibition in these patients may provide an opportunity to further reduce macular thickness and improve vision.

In summary, we show that the KKS is increased in human DME vitreous, that Klkb1 deficiency in mice decreases DM-induced RVP, and that the effects of the BK on retinal thickening do not require VEGFR2. Both B1R and B2R contribute to the effects of the KKS on retinal thickening and RVP, and these responses are mediated by eNOS and iNOS, respectively. These findings suggest that the intraocular KKS may contribute to DME via a VEGF-independent mechanism.

Acknowledgments. The authors thank Leilei Sun and Xiaohong Chen (Joslin Diabetes Center, Boston, MA) for their assistance with the proteomic analyses.

Funding. This project was supported in part by JDRF grant 17-2011-251; the Massachusetts Lions Eye Research Fund; National Institutes of Health Awards EY-019029, DK-36836, and T32-EY-007145; and Japan Society for the Promotion of Science Postdoctoral Fellowships for Research Abroad.

Duality of Interest. L.P.A. and E.P.F. are cofounders of KalVista Pharmaceuticals Ltd. The Joslin Diabetes Center holds U.S. patent 8,658,685 on methods for the treatment of kallikrein-related disorders. No other potential conflicts of interest relevant to this article were reported.

Author Contributions. T.K. designed and performed the experiments and assisted in writing the manuscript. A.C.C., N.M., and Q.Z. performed the experiments and edited the manuscript. K.F. contributed to the collection of vitreous samples. T.I. supervised the clinical work. L.P.A. contributed to the study design, reviewed the data, and edited the manuscript. E.P.F. conceived and designed the overall study, reviewed the data, and wrote the manuscript. E.P.F. is the guarantor of this work and, as such, had full access to all the data in the study and takes responsibility for the integrity of the data and the accuracy of the data analysis.

References

1. Yau JW, Rogers SL, Kawasaki R, et al.; Meta-Analysis for Eye Disease (META-EYE) Study Group. Global prevalence and major risk factors of diabetic retinopathy. Diabetes Care 2012;35:556–564

2. Klaassen I, Van Noorden CJ, Schlingemann RO. Molecular basis of the inner blood-retinal barrier and its breakdown in diabetic macular edema and other pathological conditions. Prog Retin Eye Res 2013;34:19–48

3. Klein R, Knudtson MD, Lee KE, Gangnon R, Klein BE. The Wisconsin Epidemiologic Study of Diabetic Retinopathy XXIII: the twenty-five-year incidence of macular edema in persons with type 1 diabetes. Ophthalmology 2009;116:497–503

4. Antonetti DA, Klein R, Gardner TW. Diabetic retinopathy. N Engl J Med 2012; 366:1227–1239

5. Miller JW, Le Couter J, Strauss EC, Ferrara N. Vascular endothelial growth factor a in intraocular vascular disease. Ophthalmology 2013;120:106–114

6. Aiello LP, Avery RL, Arrigg PG, et al. Vascular endothelial growth factor in ocular fluid of patients with diabetic retinopathy and other retinal disorders. N Engl J Med 1994;331:1480–1487
7. Funatsu H, Yamashita H, Ikeda T, Mimura T, Eguchi S, Hori S. Vitreous levels of interleukin-6 and vascular endothelial growth factor are related to diabetic macular edema. Ophthalmology 2003;110:1690–1696
8. Funatsu H, Yamashita H, Noma H, et al. Aqueous humor levels of cytokines are related to vitreous levels and progression of diabetic retinopathy in diabetic patients. Graefes Arch Clin Exp Ophthalmol 2005;243:3–8
9. Simó R, Sundstrom JM, Antonetti DA. Ocular Anti-VEGF therapy for diabetic retinopathy: the role of VEGF in the pathogenesis of diabetic retinopathy. Diabetes Care 2014;37:893–899
10. Elman MJ, Aiello LP, Beck RW, et al.; Diabetic Retinopathy Clinical Research Network. Randomized trial evaluating ranibizumab plus prompt or deferred laser or triamcinolone plus prompt laser for diabetic macular edema. Ophthalmology 2010;117:1064–1077, e35
11. Brown DM, Nguyen QD, Marcus DM, et al.; RIDE and RISE Research Group. Long-term outcomes of ranibizumab therapy for diabetic macular edema: the 36-month results from two phase III trials: RISE and RIDE. Ophthalmology 2013; 120:2013–2022
12. Leeb-Lundberg LM, Marceau F, Müller-Esterl W, Pettibone DJ, Zuraw BL. International union of pharmacology. XLV. Classification of the kinin receptor family: from molecular mechanisms to pathophysiological consequences. Pharmacol Rev 2005;57:27–77
13. Cicardi M, Levy RJ, McNeil DL, et al. Ecallantide for the treatment of acute attacks in hereditary angioedema. N Engl J Med 2010;363:523–531
14. Clermont A, Chilcote TJ, Kita T, et al. Plasma kallikrein mediates retinal vascular dysfunction and induces retinal thickening in diabetic rats. Diabetes 2011;60:1590–1598
15. Pouliot M, Talbot S, Sénécal J, Dotigny F, Vaucher E, Couture R. Ocular application of the kinin B1 receptor antagonist LF22-0542 inhibits retinal inflammation and oxidative stress in streptozotocin-diabetic rats. PLoS One 2012;7:e33864
16. Abdouh M, Talbot S, Couture R, Hasséssian HM. Retinal plasma extravasation in streptozotocin-diabetic rats mediated by kinin B(1) and B(2) receptors. Br J Pharmacol 2008;154:136–143
17. Catanzaro O, Labal E, Andornino A, Capponi JA, Di Martino I, Sirois P. Blockade of early and late retinal biochemical alterations associated with diabetes development by the selective bradykinin B1 receptor antagonist R-954. Peptides 2012;34:349–352
18. Liu J, Clermont AC, Gao BB, Feener EP. Intraocular hemorrhage causes retinal vascular dysfunction via plasma kallikrein. Invest Ophthalmol Vis Sci 2013; 54:1086–1094
19. Gao BB, Clermont A, Rook S, et al. Extracellular carbonic anhydrase mediates hemorrhagic retinal and cerebral vascular permeability through prekallikrein activation. Nat Med 2007;13:181–188
20. Müller F, Mutch NJ, Schenk WA, et al. Platelet polyphosphates are proinflammatory and procoagulant mediators in vivo. Cell 2009;139:1143–1156
21. Maas C, Govers-Riemslag JW, Bouma B, et al. Misfolded proteins activate factor XII in humans, leading to kallikrein formation without initiating coagulation. J Clin Invest 2008;118:3208–3218
22. Kaplan AP, Joseph K, Silverberg M. Pathways for bradykinin formation and inflammatory disease. J Allergy Clin Immunol 2002;109:195–209
23. Ma JX, Song Q, Hatcher HC, Crouch RK, Chao L, Chao J. Expression and cellular localization of the kallikrein-kinin system in human ocular tissues. Exp Eye Res 1996;63:19–26
24. Liu J, Feener EP. Plasma kallikrein-kinin system and diabetic retinopathy. Biol Chem 2013;394:319–328
25. Feener EP. Plasma kallikrein and diabetic macular edema. Curr Diab Rep 2010;10:270–275
26. Gao BB, Chen X, Timothy N, Aiello LP, Feener EP. Characterization of the vitreous proteome in diabetes without diabetic retinopathy and diabetes with proliferative diabetic retinopathy. J Proteome Res 2008;7:2516–2525
27. Gao BB, Stuart L, Feener EP. Label-free quantitative analysis of one-dimensional PAGE LC/MS/MS proteome: application on angiotensin II-stimulated smooth muscle cells secretome. Mol Cell Proteomics 2008;7:2399–2409
28. Huang W, Sherman BT, Lempicki RA. Systematic and integrative analysis of large gene lists using DAVID bioinformatics resources. Nat Protoc 2009;4: 44–57
29. Liu J, Gao BB, Clermont AC, et al. Hyperglycemia-induced cerebral hematoma expansion is mediated by plasma kallikrein. Nat Med 2011;17: 206–210
30. Xu Q, Qaum T, Adamis AP. Sensitive blood-retinal barrier breakdown quantitation using Evans blue. Invest Ophthalmol Vis Sci 2001;42:789–794
31. Liu J, Gao BB, Feener EP. Proteomic identification of novel plasma kallikrein substrates in the astrocyte secretome. Transl Stroke Res 2010; 276–286
32. Kita T, Hata Y, Miura M, Kawahara S, Nakao S, Ishibashi T. Functional characteristics of connective tissue growth factor on vitreoretinal cells. Diabetes 2007;56:1421–1428
33. Gastinger MJ, Singh RS, Barber AJ. Loss of cholinergic and dopaminergic amacrine cells in streptozotocin-diabetic rat and Ins2Akita-diabetic mouse retinas. Invest Ophthalmol Vis Sci 2006;47:3143–3150
34. Lowry JL, Brovkovych V, Zhang Y, Skidgel RA. Endothelial nitric-oxide synthase activation generates an inducible nitric-oxide synthase-like output of nitric oxide in inflamed endothelium. J Biol Chem 2013;288:4174–4193
35. Li Q, Verma A, Han PY, et al. Diabetic eNOS-knockout mice develop accelerated retinopathy. Invest Ophthalmol Vis Sci 2010;51:5240–5246
36. Nanjappa V, Thomas JK, Marimuthu A, et al. Plasma Proteome Database as a resource for proteomics research: 2014 update. Nucleic Acids Res 2014;42: D959–D965
37. Farrah T, Deutsch EW, Omenn GS, et al. A high-confidence human plasma proteome reference set with estimated concentrations in PeptideAtlas. Mol Cell Proteomics 2011;10:M110.006353
38. Sonoda S, Sakamoto T, Shirasawa M, Yamashita T, Otsuka H, Terasaki H. Correlation between reflectivity of subretinal fluid in OCT images and concentration of intravitreal VEGF in eyes with diabetic macular edema. Invest Ophthalmol Vis Sci 2013;54:5367–5374
39. Feener EP, Zhou Q, Fickweiler W. Role of plasma kallikrein in diabetes and metabolism. Thromb Haemost 2013;110:434–441
40. Bressler SB, Qin H, Beck RW, et al.; Diabetic Retinopathy Clinical Research Network. Factors associated with changes in visual acuity and central subfield thickness at 1 year after treatment for diabetic macular edema with ranibizumab. Arch Ophthalmol 2012;130:1153–1161
41. Sun JK, Lin MM, Lammer J, et al. Disorganization of the retinal inner layers as a predictor of visual acuity in eyes with center-involved diabetic macular edema. JAMA Ophthalmol 2014;132:1309–1316
42. Sun JK, Radwan S, Soliman AZ, et al. Neural retinal disorganization as a robust marker of visual acuity in current and resolved diabetic macular edema. Diabetes. 29 January 2015 [Epub ahead of print]. DOI: 10.2337/db14-0782
43. Zheng L, Kern TS. Role of nitric oxide, superoxide, peroxynitrite and PARP in diabetic retinopathy. *Front Biosci* (Landmark Ed) 2009;14:3974–3987
44. Leal EC, Manivannan A, Hosoya K, et al. Inducible nitric oxide synthase isoform is a key mediator of leukostasis and blood-retinal barrier breakdown in diabetic retinopathy. Invest Ophthalmol Vis Sci 2007;48:5257–5265
45. Zheng L, Du Y, Miller C, et al. Critical role of inducible nitric oxide synthase in degeneration of retinal capillaries in mice with streptozotocin-induced diabetes. Diabetologia 2007;50:1987–1996
46. Kim JH, Kim JH, Park JA, et al. Blood-neural barrier: intercellular communication at glio-vascular interface. J Biochem Mol Biol 2006;39:339–345
47. Ni A, Chao L, Chao J. Transcription factor nuclear factor kappaB regulates the inducible expression of the human B1 receptor gene in inflammation. J Biol Chem 1998;273:2784–2791
48. Masuda T, Shimazawa M, Hara H. The kallikrein system in retinal damage/protection. Eur J Pharmacol 2015;749:161–163